Electric-field-, temperature-, and stress-induced phase transitions in relaxor ferroelectric single crystals

Matthew Davis, Dragan Damjanovic, and Nava Setter
Ceramics Laboratory, Ecole Polytechnique Fédérale de Lausanne, Lausanne, Switzerland
(Received 25 October 2005; published 27 January 2006)

Electric-field-induced phase transitions have been evidenced by macroscopic strain measurements at temperatures between 25 °C and 100 °C in $[001]_C$-poled $(1-x)Pb(Mg_{1/3}Nb_{2/3})O_3-xPbTiO_3$ [(PMN-xPT); $x=0.25, 0.305, 0.31$] and $(1-x)Pb(Zn_{1/3}Nb_{2/3})O_3-xPbTiO_3$ [(PZN-xPT); $x=0.05, 0.065, 0.085$] single crystals. Such measurements provide a convenient way of ascertaining thermal and electrical phase stabilities over a range of compositions and give direct evidence for *first-order* phase transitions. A pseudorhombohedral (M_A)–pseudo-orthorhombic (M_C)–tetragonal (T) polarization rotation path is evidenced by *two* first-order-like, hysteretic discontinuities in strain within the same unipolar electric field cycle for PZN-5PT, PMN-30.5PT, and PMN-31PT whereas, in PMN-25PT, a single first-order-like M_A-T transition is observed. This agrees well with *in situ* structural studies reported elsewhere. Electric-field-temperature (E-T) phase diagrams are constructed showing general trends for M_A, M_C, and T phase stabilities for varying temperatures and electric fields in poled samples over the given range of compositions. The complex question of whether the M_A and M_C states constitute true phases, or rather piezoelectrically distorted versions of their rhombohedral (R) and orthorhombic (O) parents, is discussed. Finally, stress-induced phase transitions are evidenced in $[001]_C$-poled PZN-4.5PT by application of a moderate compressive stress (<100 MPa) both along and perpendicularly to the poling direction (longitudinal and transverse modes, respectively). The rotation path is likely R-M_B-O, via a first-order, hysteretic rotation within the M_B monoclinic plane. The results are presented alongside a thorough review of previously reported electric-field-induced and stress-induced phase transitions in PMN-xPT and PZN-xPT.

DOI: 10.1103/PhysRevB.73.014115 PACS number(s): 77.80.Bh, 77.80.Dj, 77.84.Dy

I. INTRODUCTION

Relaxor-ferroelectric single crystals, and especially $(1-x)Pb(Mg_{1/3}Nb_{2/3})O_3-xPbTiO_3$ (PMN-xPT) and $(1-x)Pb(Zn_{1/3}Nb_{2/3})O_3-xPbTiO_3$ (PZN-xPT), look promising as next generation actuator, sensor, and transducer materials.[1,2] Of most interest are compositions on the low $PbTiO_3$ content side of the "morphotropic phase boundary"[3,4] (MPB), where rhombohedral, orthorhombic,[5] or monoclinic[6–8] crystals poled along the nonpolar $[001]_C$ (C, pseudocubic) direction yield large anhysteretic strains <0.6%, high electromechanical coupling factors $k_{33}>0.9$, and "giant" piezoelectric coefficients $d_{33}>2000$ pm/V.[9] In terms of d_{33}, this represents a fivefold (or more) improvement over "traditional" lead zirconate titanate (PZT)-based, polycrystalline ceramics.[10]

In this paper, we report a series of unipolar, electric-field-induced strain measurements on $[001]_C$-oriented PZN-xPT ($x=0.05$, 0.065, and 0.085) and PMN-xPT ($x=0.25, 0.305$, 0.31) for temperatures between 25 °C and 100 °C, and electric fields between 0 and 1500 V/mm. Various electric-field-induced phase transitions are evidenced as (first-order-like) hysteretic, discontinuous "jumps" in strain. We discuss how such phase transitions are related to the large piezoelectric response of relaxor ferroelectric single crystals in terms of rotation of the polar vector in the $\{1\bar{1}0\}_C$ and $\{010\}_C$ mirror planes of the recently discovered M_A, M_B, and M_C monoclinic phases.[2] Electric-field-temperature (E-T) phase diagrams are constructed from the experimental data for all six compositions, which agree well with structural measurements made elsewhere; the trends for varying stability of the M_A, M_C, and tetragonal phases with changing composition around the MPB are shown. The question of the true ground state in PMN-xPT and PZN-xPT around the morphotropic phase boundary is also discussed: i.e., whether the monoclinic symmetry phases observed, both under field and in unpoled samples, are true *phases* or, rather, field-distorted versions of higher symmetry rhombohedral (R) and orthorhombic (O) parents. Finally, we evidence an analogous, *stress-induced phase transition* in $[001]_C$-oriented PZN-4.5PT by direct piezoelectric (charge-stress) measurement. Here, a pseudorhombohedral to orthorhombic phase transition can be induced by the application of a stress both along and perpendicular to the poling direction. In the latter (transverse) mode, no depolarization of the sample occurs upon unloading, behavior which will be useful for implementation of these crystals in sensing applications. It is suggested that the difference in behavior, comparing well to direct effect measurements reported previously,[11] is due to differing directions of the polarization rotation with respect to the poling direction.

Converse piezoelectric (strain-field) measurements are presented in Sec. IV A; direct piezoelectric (charge-stress) measurements are presented in Sec. IV B. In Sec. II, a thorough review of other reported electric-field-induced and stress-induced phase transitions is given in order to facilitate a full discussion of the results in Sec. IV.

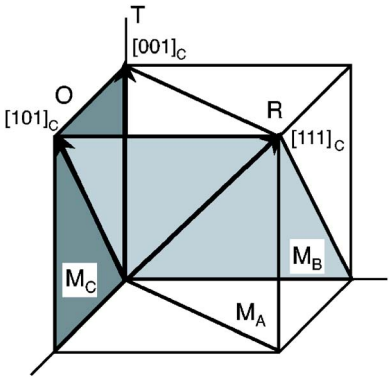

FIG. 1. (Color online) Schematic drawing of the respective $[111]_C$, $[101]_C$, and $[001]_C$ polarization directions for the rhombohedral, orthorhombic, and tetragonal phases. Also shown are the monoclinic planes $(1\bar{1}0)_C$, $(10\bar{1})_C$, and $(010)_C$ of the M_A, M_B, M_C phases, respectively. The labels M_A and M_B given here are valid only for rotations between the three limiting directions shown.

II. FIELD-INDUCED PHASE TRANSITIONS

Debate still remains over the origins of the usefully large piezoelectric properties of PMN-xPT and PZN-xPT. Much work has concentrated on precisely identifying their structure around the complicated MPB region where an orthorhombic phase[5,12,13] (O, space group $Amm2$) and two different monoclinic phases,[6,8] designated[14] M_A and M_C, have been found to exist between the tetragonal (T, space group $P4\,mm$) and rhombohedral (R, space group $R3m$) end-member phases, which lie at high and low lead titanate (PT) contents, respectively. Investigation of the MPB structure suffers from a number of complications. First, on the addition of ferroelectric lead titanate (PT) to relaxor $Pb(Mg_{1/3}Nb_{2/3})O_3$ (PMN) there is a background transition from nominally short-range ordered, relaxor behavior at low PT contents to long-range ordered, ferroelectric behavior at higher PT contents.[4,15–18] Second, the near degeneracy of the phases around the MPB means that they can often coexist within the same as-grown crystal.[7,19,20] This is aggravated by macroscopic composition heterogeneity that can result over a crystal sample[21] due to PT segregation into the melt during the crystal growth process.[22] Finally, the ground state phase in the virgin, as-grown or "zero-field-cooled" (ZFC) condition is often different to that after poling or "field cooling"[23,24] (FC). The (meta)stable state formed after poling can also differ depending on the direction of the applied electric field.[25]

In the M_A phase[14] (space group Cm), the spontaneous polarization vector is not fixed along a crystallographic direction, but, is constrained to lie in one of the dodecahedral mirror planes $\{1\bar{1}0\}_C$ of the cubic parent's point group[2] (see Fig. 1). Within this plane, it is free to lie anywhere between a $\langle 001\rangle_C$ tetragonal polar direction and a $\langle 111\rangle_C$ rhombohedral polar direction or, alternatively, anywhere between a $\langle 111\rangle_C$ and a $\langle 101\rangle_C$ orthorhombic polar direction; in the latter case, the phase is more commonly referred to as M_B, although the space group is identical.[14] In the second monoclinic phase[14] M_C (space group Pm), the remaining symmetry element is one of the cubic mirror planes $\{001\}_C$. Here, the polar vector is constrained to lie anywhere within this plane between a rhombohedral and a tetragonal polar direction (Fig. 1). In this way, M_A and M_C can be thought of as "structural bridges"[2] between the R, O, and T phases.

When the polarization vector in a monoclinic phase is close to the one of its limiting $\langle 001\rangle_C$, $\langle 101\rangle_C$, or $\langle 111\rangle_C$ directions, it can often be regarded as a slightly distorted version of that higher symmetry phase.[26] For example, in the M_C phase, if the polar vector is rotated slightly away from $[101]_C$ toward the tetragonal $[001]_C$ direction, it can be thought of as "pseudo-orthorhombic"[27,28] (although the orthorhombic phase might equally be referred to as "pseudomonoclinic"[29]). The orthorhombic phase is in fact the limiting case of M_C where two lattice parameters (a_M and c_M) of the monoclinic phase become equal;[2] this can make the two phases very difficult to resolve experimentally,[2] especially as the monoclinic distortion often tends to zero upon removal of the electric field.[29,30] Similarly, the M_A (or M_B) phase, where its polar vector is rotated away from $[111]_C$ toward $[001]_C$ (or toward $[101]_C$), can be seen as "pseudorhombohedral." There remains debate whether or not the R and M_A (and similarly the M_C and O) symmetries observed in $[001]_C$-oriented crystals constitute distinct phases,[31] as will be discussed further in Sec. IV A. However, the current consensus on the sequence of phases with increasing PT content, R-M_A (pseudorhombohedral)-M_C (pseudo-orthorhombic)-T, might not be surprising considering it mirrors exactly the R-O-T sequence of phases observed upon heating in the classical perovskites,[10] barium titanate (BT) and potassium niobate (KN). In the phenomenological theory[32,33] of PZT, a metastable orthorhombic phase can be detected close in free energy to the rhombohedral and tetragonal ground states at the MPB.

According to "polarization rotation theory,"[23] the high piezoelectric coefficients when an electric field is applied along the nonpolar $[001]_C$ direction of, say, a rhombohedral crystal is due to the ease of rotation ("inclination"[9]) of the polar vector in the mirror plane of a monoclinic phase.[2,34] Key to this theory is the concept of the *electric-field-induced phase transition*:[26,35] on the application of the field, the polarization in the lattice can rotate continuously from $[111]_C$ of the rhombohedral phase to the tetragonal $[001]_C$ direction, via the $(1\bar{1}0)_C$ "bridging"[2] plane of the M_A monoclinic phase. The phase transition sequence here would, therefore, be R-M_A-T. Many electric-field-induced phase transitions have been reported and have been evidenced both macroscopically, by measurement of polarization and strain, and microscopically by *in situ* high-resolution (neutron or x-ray) diffraction (HRD) and polarized light microscopy (PLM). They are reviewed here.

In unpoled PZN-4.5PT, upon application of an electric field along $[001]_C$, the transition R-M_A-T has indeed been observed both macroscopically[35,36] and by HRD (Ref. 29), although the jump in strain and hysteresis in the strain-electric-field (S-E) loop suggests the rotation is not continuous, i.e., it is first order in character. The same path has been observed in PMN-24PT by PLM (Ref. 37). More complicated paths have been observed by HRD, for example, in PZN-8PT (Refs. 24, 29, and 30), where the initially rhombo-

hedral crystal is transformed to the tetragonal phase via both M_A and M_C phases (and, therefore, rotations in two monoclinic planes and a jump between them). Upon removal of the field, the M_C phase[24] (or possibly orthorhombic phase[29]) is stable such that the overall rotation path is R-M_A-M_C-T-M_C and, therefore, incompletely reversible. The poled, or FC, phase in PZN-8PT is also found[24] to be M_C. Upon further field cycling of the poled crystal, the polarization follows the path M_C-T in the $(010)_C$ monoclinic plane. This rotation is itself, in fact, hysteretic and first-order-like, as evidenced by hysteretic S-E loops.[28,36] Similarly, in unpoled PMN-30PT, the path R-M_A-M_C-T has been observed for an electric field applied along $[001]_C$; here, the pseudorhombohedral M_A phase is recovered upon removal of the field,[23] and not the M_C phase as in PZN-8PT. By x-ray diffraction, Durbin *et al.* have shown that during such field-induced transitions, the macroscopic strain does indeed reflect microscopic strains in the crystal lattice[38] as expected from the "domain-engineered" structure.[9,35]

Fields applied in other directions lead to different polarization rotation paths. For PMN-30PT, with the field applied along $[101]_C$, the crystal undergoes a transition to an orthorhombic phase[25] R-M_B-O, which is characteristically anhysteretic.[39] Upon removal of the field, the M_B phase is retained.[25] Furthermore, the reverse of this path has been observed in (pseudo)orthorhombic PZN-8PT upon application of an electric field along the $[111]_C$ direction.[28] Here, a hysteretic phase transition O-M_B-R was evidenced by macroscopic measurement of strain and by polarized light microscopy, which clearly showed the nucleation and growth of the field-induced phase.

Electric-field-induced phase transitions are not unique to relaxor ferroelectrics, although the large resultant strains perhaps are. Indeed, whenever an electric field $\mathbf{E}$ is applied to a ferroelectric crystal, its polarization vector $\mathbf{P}$ will be biased by the free energy contribution[26] $-\mathbf{E}\cdot\mathbf{P}$. In tetragonal BT at room temperature, the application of an electric field along $[111]_C$ has been shown to rotate the polar vector from $[001]_C$ to the $[111]_C$ rhombohedral direction via an intermediate (pseudo)orthorhombic phase.[40] Here, the resultant strain is of the order of 0.1% compared to around 1% in PZN-xPT (Refs. 9 and 35). The same transition sequence was later replicated in the phenomenological Landau-Ginzburg-Devonshire (LGD) calculations of Bell.[26]

An externally applied, uniaxial mechanical stress σ will also bias the polar direction. On one hand, it is well known that an applied stress above some threshold level (the coercive stress) will lead to the (ferroelastic) motion of non-180° domain walls. This has been well studied in polycrystalline ceramics, especially[41] PZT, and in single crystal ferroelectrics oriented along the polar direction.[42] However, where the domain wall motion is restricted by a domain engineered configuration,[11,43] the intrinsic lattice response to a uniaxial stress can be investigated.

Work has been done on the effect of an applied prestress to the converse piezoelectric (strain-field) response of domain-engineered[44] PMN-30PT. However, to see the effect of an applied stress alone, the direct piezoelectric (charge-stress) or elastic (strain-stress) response should be investigated. Recently, the direct piezoelectric response of $[001]_C$-poled domain-engineered relaxor ferroelectric single crystals was studied.[11] Both the longitudinal and transverse direct piezoelectric effects were investigated, as shown schematically in Fig. 2, in a Berlincourt-type press. In each case, no domain wall motion is expected due to the engineered domain configuration. For a rhombohedral crystal under an applied stress along $[001]_C$, there is no driving force for domain switching between "up" and "down" domain states.[11,43] In the transverse (d_{31}) effect, where a uniaxial stress σ_1 is applied perpendicular to the poling direction, the charge density response D_3 was found to be anhysteretic; this corresponds well to the anhysteretic *converse* piezoelectric response when an electric field is applied along the $[001]_C$ direction. In contrast, the longitudinal (d_{33}) response, when a stress σ_3 is applied along the $[001]_C$ poling *direction*, was found to be hysteretic. It was postulated that different polarization rotation directions in the M_A (or M_B) monoclinic plane, one toward and one away from the $[001]_C$ poling direction, were responsible for the behavior.

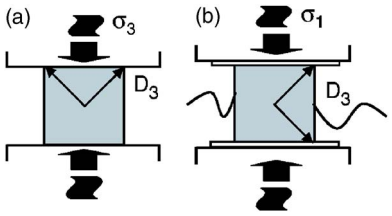

FIG. 2. (Color online) Schematic drawing of the direct (charge-stress) piezoelectric measurements in longitudinal (a) and transverse (b) modes. The arrows represent the polar vectors in the rhombohedral domain-engineered structure formed by poling along $[001]_C$.

Furthermore, by applying larger static stresses, *stress-induced phase transitions*, analogous to those induced by electric field, have been evidenced. Wan *et al.* have measured the charge-stress and strain-stress responses of PMN-32PT to a longitudinal, uniaxial stress σ_3 applied along the $[001]_C$ direction.[43] Manifest were an initial linear portion of the curve below a critical stress followed by large hysteresis and significant depolarization upon removal of the stress. In this case as well, ferroelastic switching is not expected due to the domain-engineered structure.[43] By analogy to electric-field-induced transitions, a rhombohedral to orthorhombic (or tetragonal) transition was suggested via one or more monoclinic phases. However, this has yet to be confirmed by PLM or HRD. Similarly, by applying a transverse stress along the $[001]_C$ direction in $[101]_C$-poled PMN-32PT, McLaughlin *et al.* have evidenced a rhombohedral to orthorhombic phase transition by charge-stress and strain-stress measurements.[45] Interestingly, they observed no depolarization on removal of the stress.

III. EXPERIMENTAL METHOD

The crystals used for converse (strain-field) measurements were acquired from TRS Ceramics, State College, Pennsylvania (PZN-5PT); Microfine Technologies, Singapore (PZN-

6.5PT, PZN-8.5PT); and, HC Materials, Urbana, Illinois (PMN-25PT, PMN-30.5PT, PMN-31PT). They were supplied as $10\times10\times0.5$ mm^3 plates, cut perpendicularly to the $[001]_C$ direction. Smaller samples of nominal dimensions 5×5 mm^2 were cut for measurement and gold electrodes were sputtered onto the two largest $(001)_C$ faces. Strain-field measurements were made using an optical probe system (MTI-2000 Fotonic Sensor). Electric fields were applied to the sample between a steel base plate and a copper spring contact via a high voltage amplifier. Unipolar, sinusoidal fields up to 1500 V/mm were applied at low frequency (1 Hz). Samples were poled prior to measurement by the application of 1000 V/mm for 15 min at room temperature. The steel base plate could be heated by a small oven to a maximum temperature of ~150 °C (the maximum working temperature of the optical probe). The electric field was continuously cycled for at least 30 s after stabilization of the temperature before any data were recorded.

After strain-field measurements, the permittivities of the poled samples were measured as a function of temperature while heating at 2 °C/min [zero-field heating (ZFH)]. Measurements of permittivity were then compared to equivalent data available in the literature[3,4,46,47] to verify the compositions of the crystals.

A Berlincourt-type press was used for direct piezoelectric measurements, which is described in detail elsewhere.[11,48] For measurements in the press, the boundary conditions during loading can be extremely important and low aspect (height:width) ratio samples, e.g., plates, are ill-suited.[11] Transverse stresses due to friction at the sample surfaces can reduce the d_{33} measured by as much as 30% in platelike, polycrystalline PZT samples.[49] $\langle001\rangle_C$-oriented, cuboid samples of PZN-4.5PT were thus obtained (TRS Ceramics) with dimensions $4\times4\times2$ mm^3.

For the transverse measurements, gold electrodes were sputtered onto the two largest $(001)_C$ faces. For the longitudinal measurements, the crystals were cut into two $4\times2\times2$ mm^3 columnar samples and gold electrodes were sputtered onto the two smallest 2×2 mm^2 faces. The samples were poled by applying a small field (200 V/mm) while cooling from the paraelectric phase. The samples were loaded in the press as shown schematically in Fig. 2. In the longitudinal (d_{33}) mode, a stress σ_3 is applied along the $[001]_C$-poling direction between two conducting steel plates and the charge on the two electroded surfaces (charge density D_3) is measured by a charge amplifier. In the transverse (d_{31}) mode, a stress σ_1 is applied across two opposite 4×2 mm^2 faces and the resultant charge on the electroded surfaces (D_3) is measured via two gold wires. Uniaxial stresses up to −200 MPa were applied by a stepper motor. For comparison, $\langle111\rangle_C$-oriented samples were also obtained from TRS Ceramics; they were then poled for measurement in the longitudinal mode.

IV. RESULTS AND DISCUSSION

A. Converse (strain-field) measurements

Strain-field (S-E) loops at a variety of temperatures from 25 to 100 °C, for maximum fields up 1600 V/mm, are shown in Figs. 3–8 for $[001]_C$-oriented PZN-5PT, PZN-6.5PT, PZN-8.5PT, PMN-25PT, PMN-30.5PT, and PMN-31PT. Figure 9 shows a further series of measurements taken in the high temperature, tetragonal phase of PZN-8.5PT.

It is worth noting that there is significant thermal expansion of the samples upon heating, the thermal strains being larger in general than those induced by field. However, with our experimental setup, we can only accurately make differential measurements; we do not measure the absolute reference point strain of the sample. The strains quoted here are those measured after zeroing at each new temperature. They are, therefore, purely field-induced strains for a given temperature; temperature-induced strains (thermal expansion) are not recorded. This, however, will not affect any conclusions based on the data. Only two quantities are taken from the results, a threshold electric field E_T and the strain-field gradient. Both are independent of the zero-point strain, the gradient being a differential value.

The S-E loop taken at 30 °C for PZN-5PT (Fig. 3) highlights the useful features of domain engineered relaxor ferroelectrics. The converse response is large, anhysteretic and quite linear, except for a small decrease in gradient at high field. As pointed out by Park and Shrout, the domain engineered structure formed by poling along $[001]_C$ is expected to be stable with respect to the subsequent application of a field.[9] There is no driving force for domain wall motion and the strain observed is essentially intrinsic in nature. In this way, the domain-engineered structure allows us to sample the intrinsic response of the crystals in a nonpolar direction without domain switching (excepting the fact that the very presence of domain walls in the structure, though not their motion, might augment the response[50]). The gradient of the loop ($d_{33}=dS_3/dE_3$), taken as a tangent to the curve at zero field, is 1830 pm/V. The response is similar at all temperatures up to 50 °C; d_{33} increases to 2220 pm/V over this range.

At 55 °C, however, the response has become hysteretic with the loop opening up at a threshold field $E_{T(1)}$ of around 1100 V/mm. We define this threshold field as the point at which the gradient of the lower, *rising-field* portion of the loop changes sharply (taken at the point of intersection between two tangents, as shown explicitly for the curve at 90 °C). At 65 °C, the hysteretic section is completely terminated by two linear segments, at high and low fields. The two discontinuous jumps or kinks in strain, bounding the hysteresis upon increasing and decreasing the field, are clearly now visible. Furthermore, the $E_{T(1)}$ has decreased to 740 V/mm and the zero field d_{33} has increased to 2490 pm/V. The gradient of the upper linear part of the loop is 2000 pm/V, lower than that of the lower field portion. As an aside, we note that we could define two threshold fields for this hysteresis, one on the increasing field, and one on the decreasing field. This is analogous to first-order phase transitions observed upon heating and cooling, for example, by dielectric measurement:[10] the transition temperatures in the case of such "thermal hysteresis" are different upon heating and cooling.

At 70 °C, the characteristic kink corresponding to $E_{T(1)}$ can still be weakly seen at a field of 630 V/mm. However,

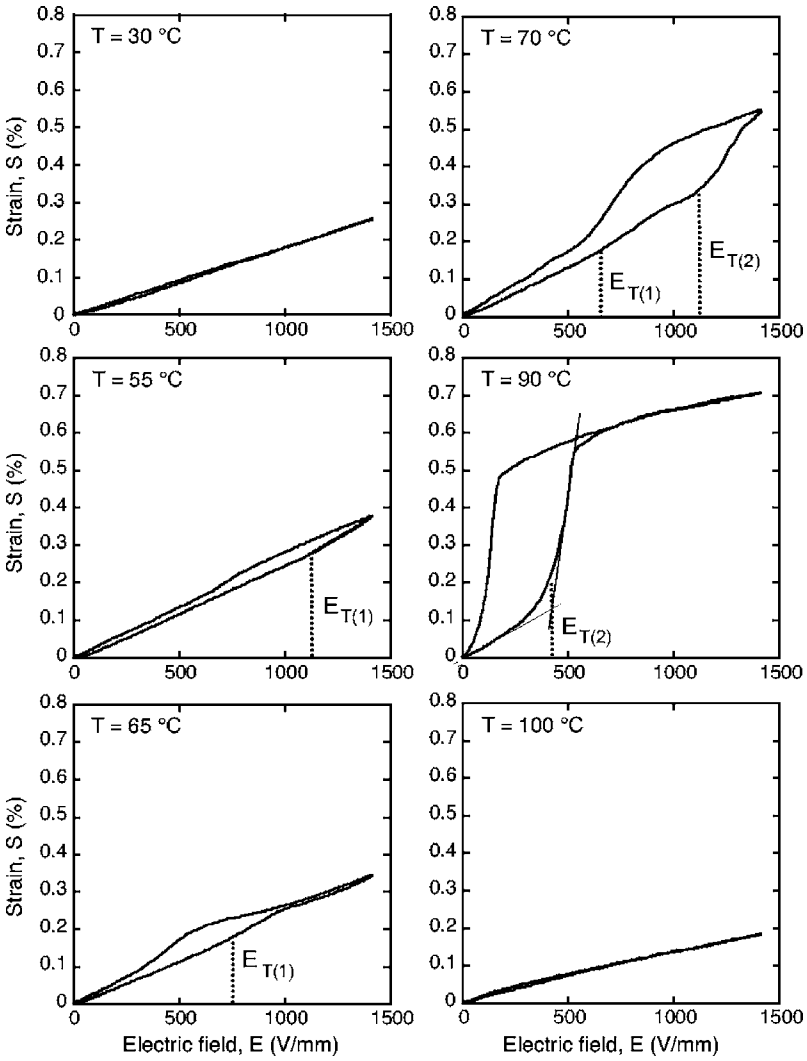

FIG. 3. Series of converse piezoelectric (strain-electric field) loops for $[001]_C$-oriented PZN-5PT, at varying temperatures between 30 °C and 100 °C. The measurements were made using an optical probe system at a frequency of 1 Hz. The threshold fields (upon increasing field) for the two electric-field-induced phase transitions, $E_{T(1)}$ and $E_{T(2)}$, are indicated by dotted lines. In each case, they are derived from a tangent-intersection construction as shown explicitly for $T=90$ °C.

there is now a second discontinuity in strain, occurring after the first, at a threshold field $E_{T(2)}$ of around 1100 V/mm. An even bigger hysteresis is observed, and the accompanying strain is higher, reaching around 0.55%. It is worth noting here that the appearance of two discontinuities in the same strain-field cycle is even clearer for PMN-30.5PT (Fig. 7, 55 °C) and PMN-31PT (Fig. 8, 45 °C), where the two threshold fields are further separated.

At 90 °C, the first discontinuity can no longer be seen, though the second hysteresis can be seen to terminate completely. The threshold field for the second transition $E_{T(2)}$ has dropped to around 400 V/mm. Again, the high field portion of the loop after the hysteresis is linear. The gradient is 1160 pm/V at maximum field compared to 3100 pm/V before the transition at zero field.

Finally, at 100 °C, no discontinuity can be seen. The response is again anhysteretic and linear with a gradient d_{33} (at high field) of 1190 pm/V.

The behavior can be attributed to two electric-field-induced phase transitions, as follows. At 30 °C, the crystal is rhombohedral in its ground state. Initial application of an electric field along $[001]_C$ (poling) will lead to a rotation of the polar vector away from the $[111]_C$ polar direction in the $(1\bar{1}0)_C$ plane. This piezoelectric[31] distortion must break the rhombohedral symmetry and result in M_A symmetry. When the field is removed, the crystal will either revert back to its rhombohedral ground state or remain in a field-distorted, pseudorhombohedral M_A state; whether or not this constitutes a new monoclinic ground state (zero field) *phase* will be discussed later in this section. Upon further field cycling, below a critical field $E_{T(1)}$, the rotation in the M_A plane is continuous and reversible.

Since no domain wall motion is expected due to the stable, domain-engineered configuration,[9] the two discontinuities in the strain-field loops at higher temperatures reflect discontinuities in the lattice strain[38] and, correspondingly, discontinuous rotations of the polar vector in its path toward $[001]_C$. The discontinuous strain and accompanying hysteresis, implying metastable phases over a finite range of fields, are evidence of a first-order, electric-field-induced phase transition (EFIPT). In contrast, the anhysteretic, closed sections of the loops observed before such transitions suggest continuous polarization rotations within a single monoclinic plane. The gradient of each linear section represents the piezoelectric coefficient d_{33} associated with the corresponding rotation and is essentially constant over that field range.

The first EFIPT, observed (for the field applied) above 55 °C, is gentle, involving a relatively small jump in strain

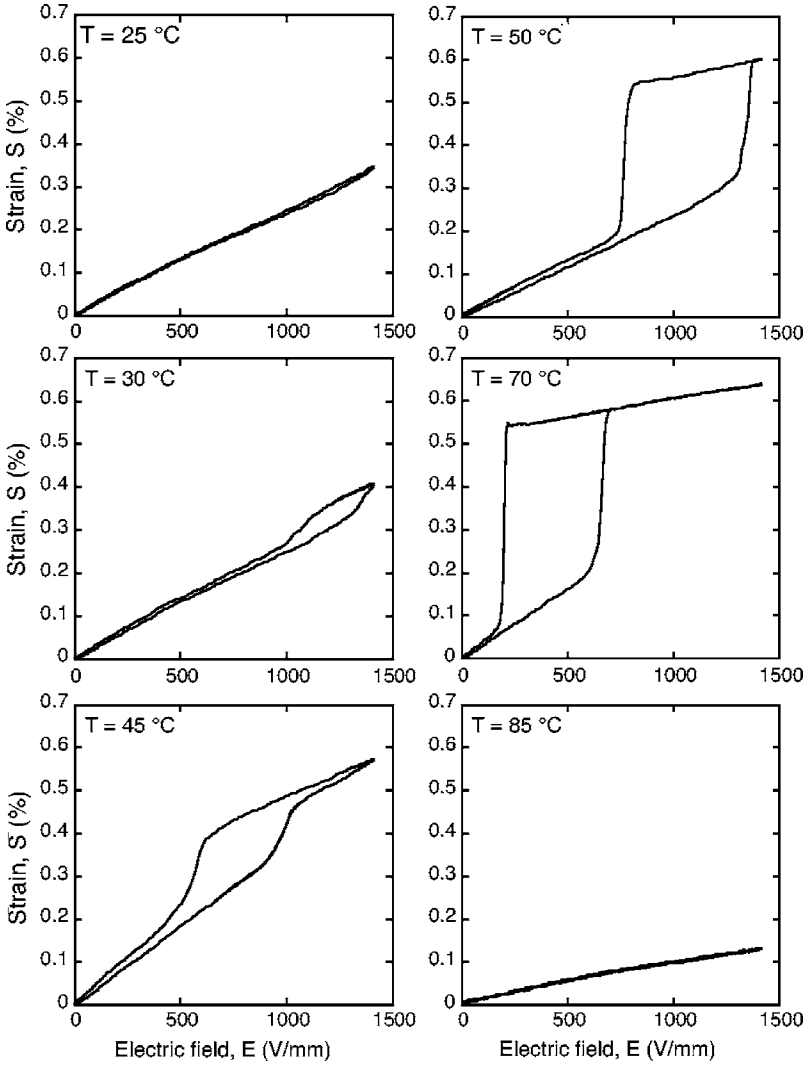

FIG. 4. Series of converse piezoelectric (strain-electric field) loops for $[001]_C$-oriented PZN-6.5PT, at varying temperatures between 25 °C and 85 °C. The measurements were made using an optical probe system at a frequency of 1 Hz.

and only a small decrease in the gradient of the strain-field loop. According to HRD work presented elsewhere,[23] the first transition will correspond to a jump from the $(1\bar{1}0)_C$ to the $(010)_C$ monoclinic plane, therefore, representing a transition from M_A to pseudo-orthorhombic M_C symmetry. The gradient of the low field section, d_{33}=2490 pm/V, corresponds to rotation in the M_A plane; the smaller gradient of the second linear portion, d_{33}=2000 pm/V, represents a slightly harder polarization rotation in the M_C plane.

The second EFIPT involves a noticeably more severe jump in strain. By comparison to HRD results[24] for PZN-8PT, we assign this transition to one between M_C and the final tetragonal phase. At fields just before the transition, and larger than $E_{T(1)}$, there is a continuous polarization rotation in the M_C plane. At $E_{T(2)}$, however, there is a second discontinuous jump in strain, within the M_C plane, to a T phase; the jumps in strain and hysteresis again suggest a first-order-like transition.

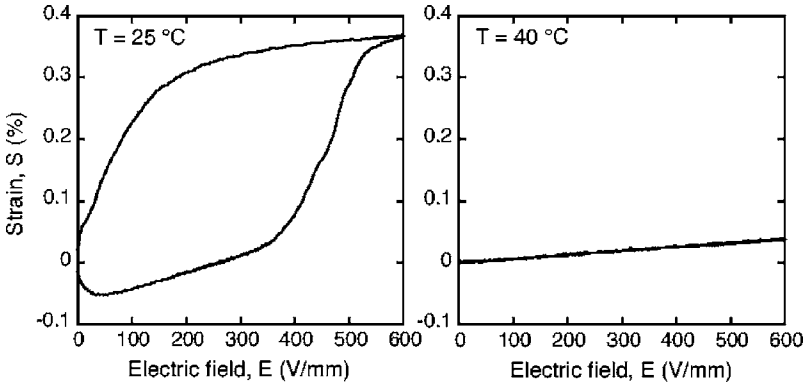

FIG. 5. Converse piezoelectric (strain-electric field) loops for $[001]_C$-oriented PZN-8.5PT, at 25 °C and 40 °C. The measurements were made using an optical probe system at a frequency of 1 Hz.

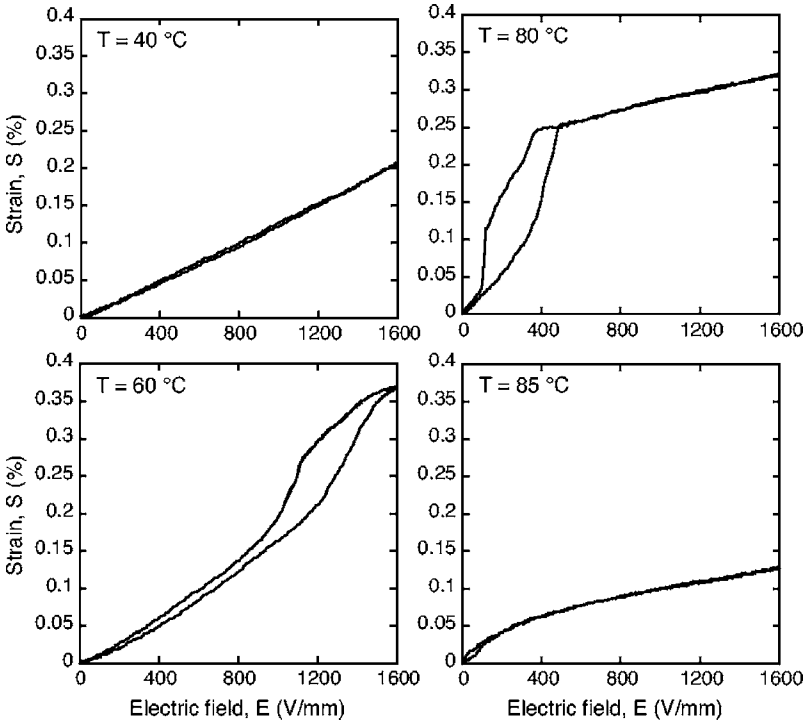

FIG. 6. Series of converse piezoelectric (strain-electric field) loops for $[001]_C$-oriented PMN-25PT, at varying temperatures between 40 °C and 85 °C. The measurements were made using an optical probe system at a frequency of 1 Hz.

Overall the polarization rotation path is M_A-M_C-T and involves two first-order-like, discontinuous phase transitions, one between monoclinic planes M_A-M_C, and one within the M_C plane to the tetragonal phase. The strain-field loops for PZN-6.5PT (Fig. 4), PMN-30.5PT (Fig. 7) and PMN-31PT (Fig. 8) follow the same path. The two EFIPTs can be clearly seen within the same strain-field loop for PMN-30.5PT (Fig. 7, 55 °C) and PMN-31PT (Fig. 8, 45 °C). This suggests that the transition sequence is completely reversible in so far as a pseudorhombohedral phase (R or M_A) is retained at zero field.

The zero-field gradient d_{33} for PZN-6.5PT is shown as a function of temperature in Fig. 10. For different temperature ranges, the piezoelectric coefficients correspond to polarization rotations in the M_A or M_C monoclinic planes, as marked on the graph, or to collinear polarization extension in the tetragonal phase T. In each case, d_{33} increases with increasing temperature especially close to temperature-induced phase transitions where $E_{T(1)}$ and $E_{T(2)}$ decrease to zero. The largest d_{33} is found for the M_A rotation; d_{33} is slightly smaller for the M_C rotation, though it is still above 2000 pm/V. In the tetragonal phase, where the application of the field along the polar $[001]_C$ leads to a uniquely collinear[51] piezoelectric effect, d_{33} is characteristically much weaker. That the piezoelectric coefficient is much larger for fields applied in nonpolar directions is common to many ferroelectric perovskites,[52] especially when a ferroelectric-ferroelectric phase transition is approached.

In PZN-8.5PT, the behavior is different, as shown in Fig. 5. At 25 °C, the strain-field loop is already hysteretic; there is no linear portion of the curve and the initial negative strain observed on increasing field shows that the sample is at some metastable point within the hysteresis loop. $[001]_C$-poled PZN-8PT is known to be pseudo-orthorhombic (M_C or O) at room temperature[24] and very close in energy to the neighboring tetragonal phase. Here, therefore, the hysteresis corresponds to the M_C-T EFIPT. The threshold field at 25 °C is small, $E_{T(2)}$=380 V/mm, reflecting the near degeneracy of the M_C and T phases in PZN-8.5PT at room temperature. At 40 °C, the sample is tetragonal at the zero field.

As an aside, it is worth noting that the tetragonal phase is no longer domain engineered with respect to a field applied along the $[001]_C$ direction. Therefore, some domain wall motion might be expected, especially if the monodomain state is not stable at zero fields (as observed elsewhere for rhombohedral[53] PMN-33PT). The 90° domain wall motion would be manifest in the strain-field response as hysteresis, which it indeed is at higher temperatures. As the temperature is increased in the tetragonal phase, the hysteresis caused by 90° domain wall motion actually increases in its maximum strain (see Fig. 9), although the coercive field is almost constant. Tetragonality in the T phase $(c_T-a_T)/a_T$ (where a_T and c_T are the unit cell parameters in the T phase) actually decreases with temperature toward the cubic phase.[24] It, therefore, appears that more domain walls can switch at higher temperatures, where tetragonality is smaller. Finally, it should be noted that the hysteretic strains due to ferroelastic switching are much smaller than those due to phase transitions in the lattice. Similar domain switching behavior under unipolar fields has been observed at room temperature for $[101]_C$-oriented orthorhombic[28] PZN-8PT and $[111]_C$-oriented rhombohedral[35] PZN-4.5PT.

The response of PMN-25PT, deep in the rhombohedral phase field,[4,7] is again different (see Fig. 6). In this sample, only one transition was observed and at much higher temperatures and fields. Since the induced phase is characteristically tetragonal (with a weak d_{33}=710 pm/V at 80 °C), it seems that there is a direct pseudorhombohedral-tetragonal EFIPT via a discontinuous, first-order-like rotation in the M_A monoclinic plane. The same path has been observed in both

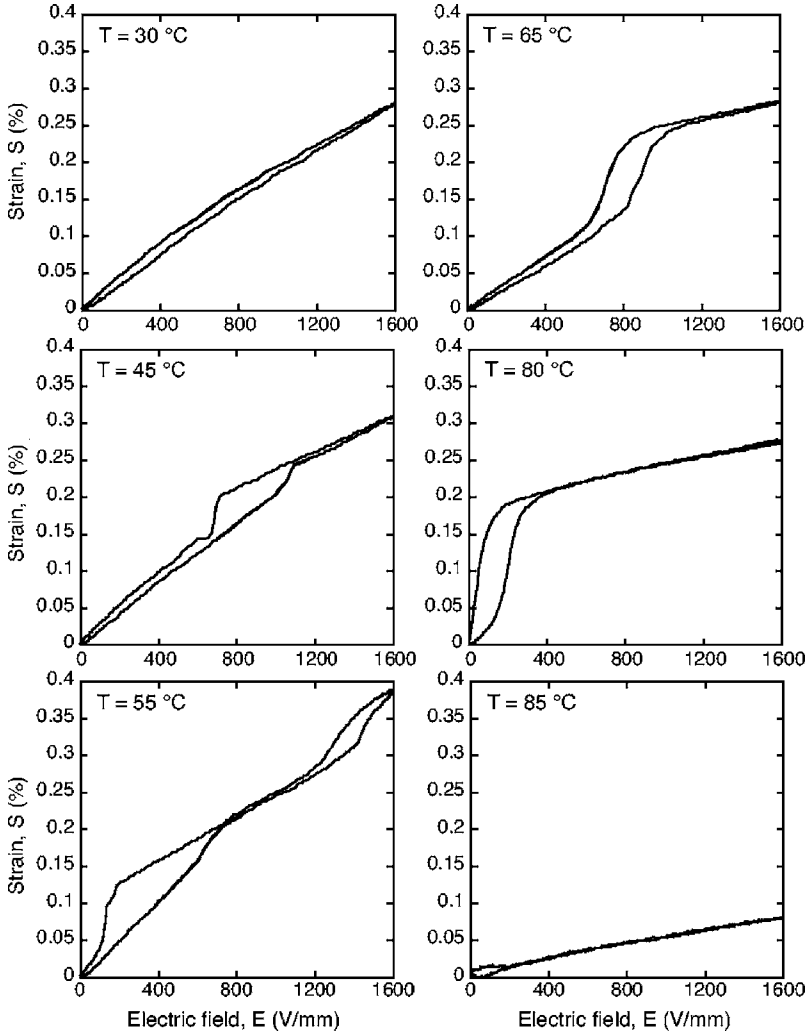

FIG. 7. Series of converse piezoelectric (strain-electric field) loops for $[001]_C$-oriented PMN-30.5PT, at varying temperatures between 30 °C and 85 °C. The measurements were made using an optical probe system at a frequency of 1 Hz.

rhombohedral PZN-4.5PT by macroscopic strain-field measurements[36] and HRD (Ref. 29) and in rhombohedral[37] PMN-24PT by PLM. There is no evidence of a transition to the second, M_C monoclinic plane in this composition.

Importantly, both fields $E_{T(1)}$ and $E_{T(2)}$ are functions of temperature. If the threshold field for one EFIPT is higher than the maximum field applied, it will not occur. If the threshold field for an EFIPT becomes zero at higher temperatures, i.e., if a temperature-induced phase transition to a new ground state takes place, it will also not appear. Therefore, to summarize the results, electric-field-temperature (E-T) phase diagrams have been constructed based on plots of the threshold fields $E_{T(1)}$ and $E_{T(2)}$ as a function of temperature; they show the various phase stabilities of each composition, after poling, for electric fields applied along $[001]_C$. The E-T phase diagrams are shown in Fig. 11 for PMN-xPT [$x=0.25,0.305,0.31$; (a)–(c), respectively] and PZN-xPT [$x=0.05,0.065,0.085$; (d)–(f)]. Where the threshold field was difficult to judge from the S-E curves, i.e., where the threshold field was close to zero or where the two phase transitions occurred very close together, they have been omitted. The phase fields are designated M_A, M_C, and T and refer to the symmetry under nonzero fields applied along the $[001]_C$ direction. The true ground (or zero-field) phase will be discussed later.

Various trends can be seen from the graphs. In general, with increasing temperature and/or electric field along $[001]_C$, the sequence of phases is M_A-M_C-T. The temperatures and field levels of the M_A-M_C and M_C-T transitions for PMN-30.5PT agree qualitatively well with those found by Bai *et al.* by *in situ* x-ray diffraction upon application of an electric field[23] to PMN-30PT. There, the M_C phase is favored by higher fields: notice the widening of the M_C "triangle" in graphs (b)–(e) in Fig. 11. Moreover, it is also favored by higher PT contents. The M_C triangle noticeably decreases in width on lowering PT content [Figs. 11(c) and 11(b)] and is eventually squeezed out at very low PT contents. In PMN-25PT [Fig. 11(a)], it no longer appears, and in PZN-5PT [Fig. 11(d)], it is very narrow at low fields. As reported elsewhere, no M_C phase is observed at any field level[29] in PZN-4.5PT. Measurements by Ren *et al.* on PZN-4.5PT evidence only one first-order-like EFIPT[36] upon application of an electric field along $[001]_C$ at temperatures between 25 °C and 105 °C. This all suggests that the M_C triangle is also "squeezed out" in PZN-4.5PT, as observed here for PMN-25PT, and that the M_A-T path is followed. However, it has also been suggested that a small range of M_C phase stability persists to even lower PT contents,[54] although perhaps the phase field becomes so small as to be experimentally insignificant. Finally, the M_C triangle is driven to lower tempera-

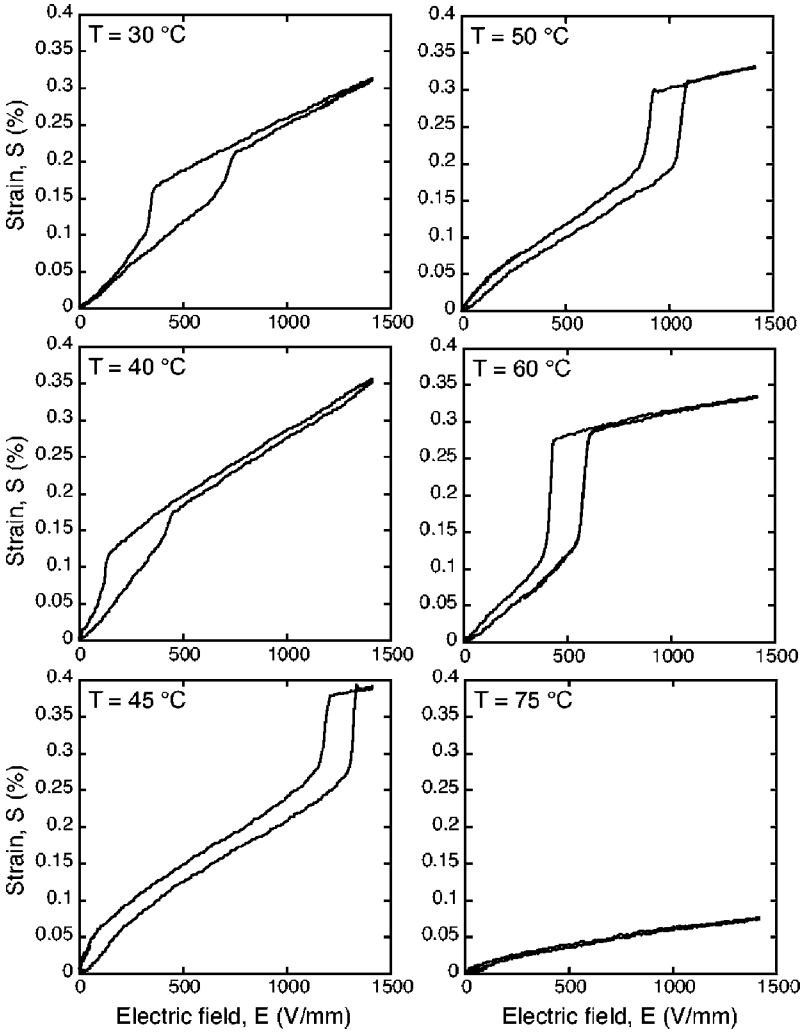

FIG. 8. Series of converse piezoelectric (strain-electric field) loops for $[001]_C$-oriented PMN-31PT, at varying temperatures between 30 °C and 75 °C. The measurements were made using an optical probe system at a frequency of 1 Hz.

tures with increasing PT content. In PZN-8.5PT, at room temperature, only the M_C-T EFIPT is observed. Such E-T phase diagrams will be helpful in terms of electrical and thermal stability for the use of PZN-xPT and PMN-xPT single crystals in high voltage applications.

Finally, we turn our attention to the question of the ground state phase. In terms of a purely classical, sixth order LGD expansion of the free energy, monoclinic phases cannot exist at zero stress or the zero electric field. Only the rhombohedral, orthorhombic, and tetragonal phases are generated, stably or metastably, in the phenomenological theories of barium titanate[26,52] and PZT (Ref. 32) with polar vectors along the $\langle 111\rangle_C$, $\langle 101\rangle_C$, or $\langle 001\rangle_C$ directions, respectively. Application of an electric field along the polar direction of either phase itself can only lead to the elongation of the polar vector **P** (the collinear piezoelectric effect), which is characteristically weak.[55] However, upon application of an electric field along a $\langle 111\rangle_C$, $\langle 101\rangle_C$, or $\langle 001\rangle_C$ direction away from

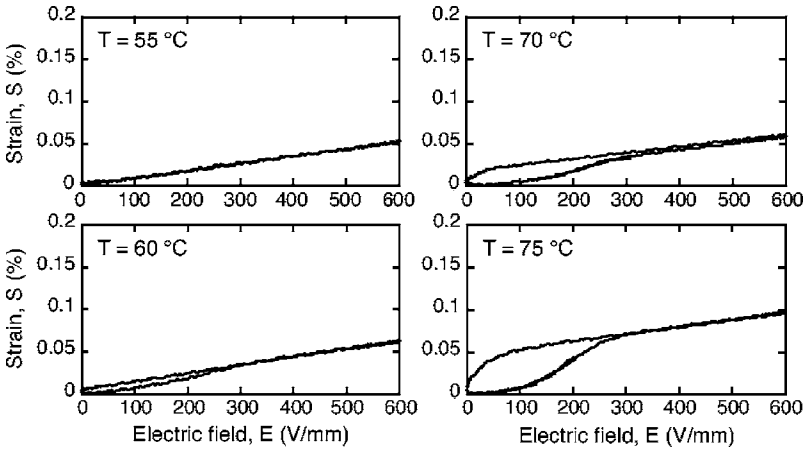

FIG. 9. Series of converse piezoelectric (strain-electric field) loops for $[001]_C$-oriented PZN-8.5PT, at varying temperatures between 55 °C and 75 °C, in the high temperature tetragonal phase. The measurements were made using an optical probe system at a frequency of 1 Hz. The hysteretic response is due to ferroelastic (90° domain) switching.

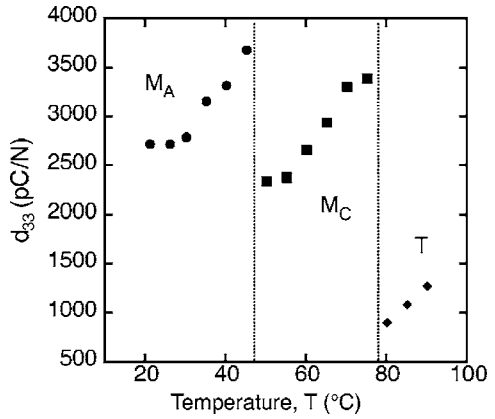

FIG. 10. d_{33} as a function of temperature for $[001]_C$-oriented PZN-6.5PT derived from the strain-field (S-E) measurements shown partially in Fig. 4. d_{33} is taken as the gradient of the S-E loop at the zero field. At high temperatures in the tetragonal phase, d_{33} corresponds to the collinear extension of the polar vector. At lower temperatures, d_{33} corresponds to rotation in either the M_A or M_C monoclinic plane, as marked.

the polar direction of the respective R, O, or T phase, the polarization vector will rotate toward that direction. This is the physical meaning of the piezoelectric shear coefficients, which are characteristically large close to ferroelectric-ferroelectric phase transitions due to dielectric softening perpendicular to the polar vector;[52] this includes proximity[52] to a MPB. Most importantly, this polarization rotation will break the symmetry of the higher symmetry ferroelectric phase. As described in the Introduction, if a field is applied along $[001]_C$ to a rhombohedral crystal, the $[111]_C$ polar vector will rotate, within the M_A monoclinic phase, toward $[001]_C$. The rhombohedral symmetry is immediately broken and the sole remaining symmetry element will be the M_A monoclinic plane bridging the $[111]_C$ and $[001]_C$ directions. Critically, as pointed out by Kisi *et al.*, this can simply be regarded as a piezoelectric distortion and in fact not a phase transition.[31] From this point of view, the induced M_A "phase" is not a true phase and should be better labeled a monoclinic "distortion." All M_A, M_B, and M_C monoclinic *distortions* become possible by permutating the three R, O, and T ground states with the three $\langle 111\rangle_C$, $\langle 101\rangle_C$, and $\langle 001\rangle_C$ directions of the applied field[26] within the framework of sixth-order LGD theory.

The question, therefore, arises, whether or not the rotation that occurs at infinitesimally small electric fields (or stresses) corresponds to a true phase transition. This can be examined by considering the *order* of the phase transition. Second-order transitions are characterized by a continuous change in the order parameter, polarization **P** in the case of ferroelectrics, whereas first-order phase transitions involve a discontinuity. First-order transitions are characteristically hysteretic due to the coexistence of metastable phases; in contrast, second-order transitions should be thermodynamically anhysteretic. Forrester *et al.*[56] and Sergienko *et al.*[57] point out that, according to the group-theory-based Landau condition,[58] phase transitions between the rhombohedral phase and the M_A, M_B, and M_C monoclinic phases cannot be second-order (whereas $O \leftrightarrow M_B$, $O \leftrightarrow M_C$, $T \leftrightarrow M_C$, and $T \leftrightarrow M_A$ transitions can be first or second order[57]). There is no general argument that forbids a first-order phase transition.[57] It follows that there can be no continuous rotation of the polar vector from the R to the M_A *phase*; where there is a continuous rotation, evidenced, for example, by the absence of hysteresis, the field-induced structure should be described as a monoclinic distortion.

Confusingly, in the first-principles calculations of Bellaiche *et al.* for rhombohedral PZT near the MPB, the application of an electric field along $[001]_C$ does lead to a discontinuous jump in strain between R and M_A phases indicating a true, first-order phase transition.[59] However, it was not reported in the first-principles calculations of Fu and Cohen for low temperature, rhombohedral barium titanate for the same applied field direction, where the same R-M_A rotation is predicted.[34] In the *in situ* HRD work of Bai *et al.* on $[001]_C$-oriented[23] PMN-30PT, an R-M_A transition is discussed, although the nature of the evolution of the lattice constant through the transition (whether continuous or discontinuous) is not presented. Similar work by the same authors on unpoled, $[101]_C$-oriented[25] PMN-30PT does not show clearly the nature of the corresponding R-M_B transition at low fields.

When higher (eighth) order terms are added to the LGD expansion, zero-field monoclinic phases are predicted by phenomenological theory.[14] Experimentally, both M_A (M_B) and M_C monoclinic phases have been found to exist in as-grown, unpoled, or zero-field cooled samples of PMN-xPT by both HRD (Ref. 6) and PLM (Refs. 7, 60, and 61). In these studies, the rhombohedral phase is observed only at lower PT contents ($x \leqslant 0.26$).[6] Furthermore, monoclinic phases have also been found to exist in samples after the removal of an electrical field or in the field-cooled condition. For instance, after the removal of a field applied along $[001]_C$ to initially rhombohedral PMN-30PT, the M_A phase is stable;[23] when the field is applied along $[101]_C$ and removed, the M_B phase remains.[25]

The question remains, whether or not these monoclinic phases are the true ground state, zero-field equilibrium phases near the MPB in PMN-xPT and PZN-xPT and, if so, whether their presence is directly responsible for the usefully large piezoelectric response, as is often assumed. Suggestions have been made that the presence of the monoclinic phase after high field poling is due to remnant tetragonal domains which strain the rhombohedral regions.[62] That is, residual stresses due to the coexistence of nonelastically matched phases are responsible for the monoclinic distortion. In Sec. IV B, we give indirect evidence of a rhombohedral to orthorhombic phase transition, via a monoclinic phase, under an applied stress. The monoclinic distortion as a "trapped metastable phase" has also been suggested.[63] Furthermore, a theoretical treatment[64] has shown that the presence of a monoclinic plane has an important role in relieving stress in samples where two phases coexist together in the same sample. Such two phase coexistence is often observed in unpoled PMN-xPT and PZN-xPT near the MPB (Refs. 7, 19, and 20). As well as internal stresses, internal electric fields might also be responsible for the presence of monoclinic

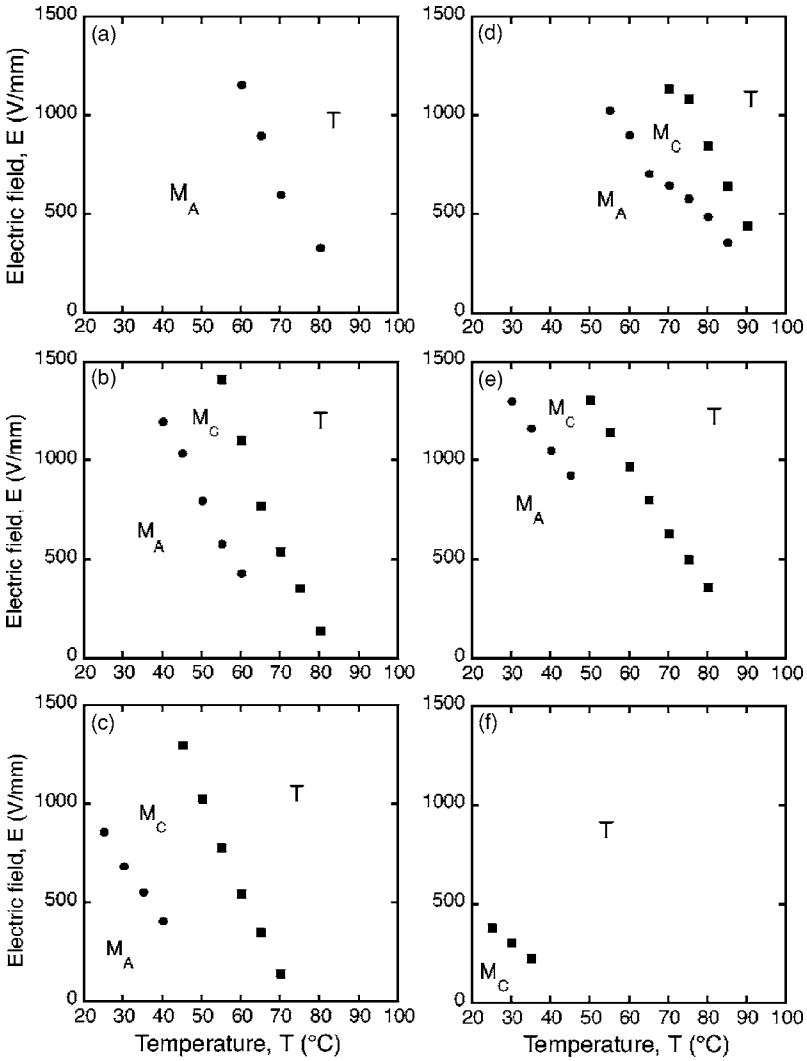

FIG. 11. Electric-field-temperature phase diagrams, derived from the strain-field loops shown in Figs. 3–8, for (a) PMN-25PT, (b) PMN-30.5PT, (c) PMN-31PT, (d) PZN-5PT, (e) PZN-6.5PT, and (f) PZN-8.5PT. The phase fields are marked with the symmetry of the phase under finite field.

phases in the poled state. For example, an internal bias field ("memory") has been found to develop upon field cooling in $[001]_C$-oriented PZN-8PT, possibly due to the alignment of defect dipoles;[65] this might also contribute to a remnant monoclinic distortion. The presence of charged domain walls[66] in the domain-engineered structure, where uncompensated by mobile point charges, will also lead to internal fields. Interestingly, Jin *et al.* have proposed a model for the monoclinic and orthorhombic phases in PMN-*x*PT and PZN-*x*PT as symmetry adaptive phases, built up of tetragonal or rhombohedral microdomains;[67] here, the domain-averaged symmetry can be orthorhombic or monoclinic depending on the nanoscale twinning of the domains.

Moreover, all the above discussion also ignores the background relaxor nature of PMN-*x*PT and PZN-*x*PT and, therefore, the presence of random fields due to B-site cationic disorder. In the related solid solution PZT, the need for B-site disorder in stabilizing the M_A phase at the MPB has been discussed.[68,69] Moreover, in the solid solution $(1-x)PbSc_{1/2}Nb_{1/2}O_3-xPbTiO_3$ (PSN-*x*PT), which exhibits a MPB similar to PMN-*x*PT and PZN-*x*PT, first-principles calculations suggest that the M_C monoclinic plane is promoted by the presence of nanoscale chemically ordered regions at higher PT contents, whereas the M_A phase is due to homogeneous B-site disorder.[70]

Monoclinic distortions will also occur in classical perovskites, as shown phenomenologically for barium titanate.[26] That is, polarization rotation is not unique to relaxor ferroelectrics. However, zero-field monoclinic phases are not observed in barium titanate and potassium niobate, although they are in PZT near the morphotropic phase boundary.[71] As mentioned in the Introduction, the application of a field along $[111]_C$ to the tetragonal phase of barium titanate results in the polarization path *T*-*R* via two intermediate monoclinic symmetry phases.[26,40] Budimir *et al.* have pointed out that piezoelectric shear coefficients and, therefore, the polarization rotation effect become stronger in all perovskites close to ferroelectric-ferroelectric (FE-FE) phase transitions.[52] This is true of FE-FE transitions induced by changes in both temperature and composition;[52] indeed the increase in piezoelectric shear coefficient toward the MPB has been predicted using phenomenological theory by many authors.[32,57,72] Importantly, the size of *all* piezoelectric coefficients is much smaller in barium titanate and other classical perovskites[52] than in PZT, and especially PMN-*x*PT and PZN-*x*PT; this is related to the fact that PZN-*x*PT and PMN-*x*PT are around nine times softer elastically than other

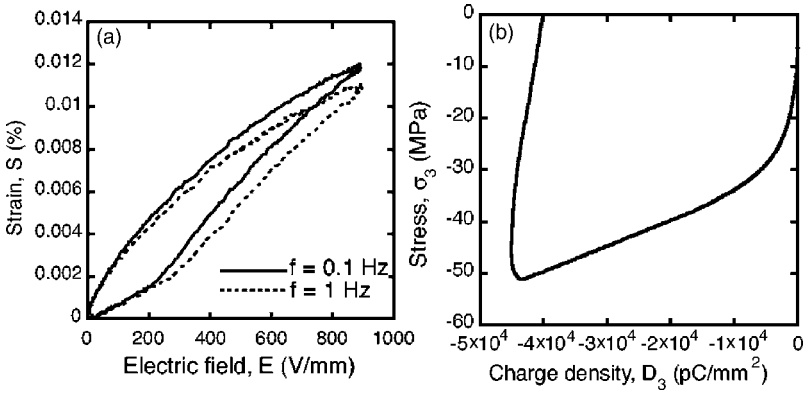

FIG. 12. (a) Unipolar strain-electric-field loop for a (poled) sample of $[111]_C$-oriented PZN-4.5PT measured using an optical probe system. (b) Subsequent direct piezoelectric (charge-stress) response of the same sample upon application of a uniaxial compressive stress along the $[111]_C$ direction.

piezoelectric perovskites.[31] As a consequence, the monoclinic distortion itself will be much smaller in the simpler perovskites and, therefore, more difficult to detect. Therefore, the question remains, are the monoclinic phases really responsible for the large piezoelectric response in PMN-xPT and PZN-xPT? Or, alternatively, might the presence of the monoclinic phases in nominally ground state PZN-xPT and PMN-xPT be due to their large piezoelectric response to small perturbing fields, including residual stresses, and internal electrical bias fields due to defects, charged domain walls, and so forth? Critically, better *in situ* diffraction evidence of the R-M_A transition, and likewise the O-M_C transition, is needed to establish whether these transitions really correspond to true, first-order phase transitions or rather piezoelectric distortions. Unfortunately, this will be difficult experimentally due to the witheringly small lattice distortions involved.

Irrespective of the ground state and whether M_A and M_C observed are true phases or field-induced distortions of a higher symmetry phase, it is certainly the polarization rotations in the M_A and M_C monoclinic planes that are responsible for the giant piezoelectric response of PMN-xPT and PZN-xPT single crystals when a field is applied along the $[001]_C$ direction. In any case, for poled samples under nonzero $[001]_C$ fields, the symmetry will always be monoclinic or tetragonal. The polarization rotations are continuous except for the first-order, electric-field-induced phase transitions that occur between M_A and M_C monoclinic planes, within the M_C monoclinic plane (M_C-T) and, for low PT contents, within the M_A monoclinic plane (M_A-T). All three of these transitions have been evidenced here by macroscopic strain-field measurement. They are characteristically hysteretic, involving large discontinuous jumps in strain, and occur at transition fields that are strong functions of temperature and composition. That these transitions between pseudorhombohedral, pseudo-orthorhombic, and tetragonal phases occur at such small electric fields is a direct consequence of their near degeneracy, especially close to the morphotropic phase boundary at room temperature. In Sec. IV B, we show how analogous phase transition behavior can be induced by the application of mechanical stress.

B. Direct (charge-stress) measurements

The longitudinal charge-stress response of $[111]_C$-oriented PZN-4.5PT is shown in Fig. 12(b). Alongside, in Fig. 12(a), is shown the converse strain-field response measured on the same sample. The converse response was measured first, since the application of a compressive stress will depole the sample. PZN-4.5PT is rhombohedral in its ground state[29] and, therefore, when poled along $[111]_C$, cannot have a domain-engineered structure. The piezoelectric response on application of an electric field along $[111]_C$ corresponds to the collinear effect. It is characteristically weak with $d_{33} \sim 80$ pC/N measured at small field. Moreover, it is hysteretic due to ferroelastic (non-180°) domain wall motion in the absence of domain engineering. Similar results have already been reported elsewhere for $[111]_C$-oriented, rhombohedral[35] PZN-4.5PT, and PMN-xPT ($x=0.28$ and 0.33),[28] and the loop shown here is qualitatively similar to the response of the non-domain-engineered, tetragonal phase to fields along $[111]_C$ described in Sec. IV A (Fig. 9). The coercive (switching) field is notably frequency-dependent as observed in bipolar switching loops.[73]

The charge-stress loop [Fig. 12(b)] also exhibits a large hysteresis. Upon unloading, the crystal is significantly depoled with a net depolarization of $\Delta D_3 = -0.04$ C/m^2. This behavior is characteristic of ferroelastic switching as observed both in (soft) PZT ceramics[41] and non-domain-engineered, single crystal barium titanate, oriented along the polar $[001]_C$ direction.[42] We, therefore, explain the hysteresis and depolarization observed in rhombohedral, $[111]_C$-oriented PZN-4.5PT by global, ferroelastic (70.5° or 109.5°) switching driven by the application of a uniaxial, compressive stress.

$[001]_C$-poled, rhombohedral PZN-4.5PT, however, is domain engineered. As stated in the Introduction, for the application of an electric field or a compressive stress along the poling direction, there is no driving force for domain wall motion.[11,43] As expected, very different behavior is observed for $[001]_C$-oriented PZN-4.5PT in the direct piezoelectric effect.

Figure 13(a) shows the transverse ($D_3 - \sigma_1$) response of $[001]_C$-oriented PZN-4.5PT; Fig. 13(b) shows the longitudinal ($D_3 - \sigma_3$) response. In the transverse mode (a), the curve is linear at low stresses with a reciprocal gradient ($d_{31} = dD_3/d\sigma_1$) of −1290 pC/N. After a threshold stress of −15 MPa, there are two kinks in the curve and an obvious hysteresis before a second, nearly linear, section at high stress. The gradient at maximum compressive stress (d_{31}) is −170 pC/N. The loop is completely closed, indicating its

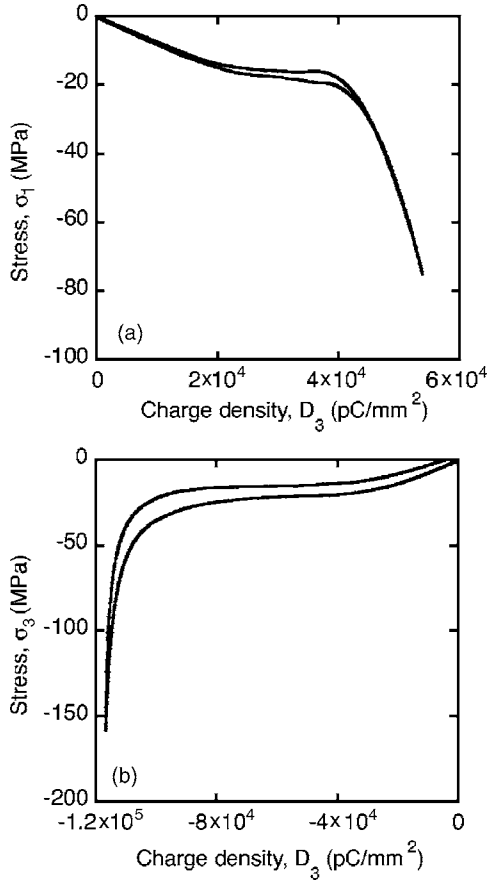

FIG. 13. Quasistatic, direct piezoelectric (charge-stress) measurements on a sample of $[001]_C$-oriented PZN-4.5PT. In the transverse mode (a), a uniaxial compressive stress σ_1 is applied along $\langle 100\rangle_C$ perpendicular to the poling direction and the charge density along the $[001]_C$-poling direction D_3 is measured; the reciprocal gradient is a measure of d_{31}. In the longitudinal mode (b), a uniaxial compressive stress σ_3 is applied along the $[001]_C$-poling direction, and the charge density D_3 is measured; the reciprocal gradient is a measure of d_{33}.

complete reversibility, with zero depolarization.

The longitudinal response [Fig. 13(b)] is also initially linear with a reciprocal gradient at zero stress of around $d_{33}=1550$ pC/N. As the stress is increased, the reciprocal gradient of the curve increases sharply at a threshold field of around −20 MPa. At high stresses, the response saturates and exhibits a very small reciprocal gradient of $d_{33}<30$ pC/N. Upon unloading, the curve is hysteretic at all stresses and the loop does not close. The depolarization, reproducible for subsequent cycles, is around $\Delta D_3=-0.005$ C/m^2.

The longitudinal response shown in Fig. 13(b) is qualitatively similar to that observed elsewhere for $[001]_C$-oriented[74] PMN-30PT and PMN-33PT, and PMN-32PT (Ref. 43). In the relevant loops reported by Wan *et al.* (PMN-30PT) and Feng *et al.* (PMN-30PT, PMN-33PT), there is an initial linear portion of the curve for stresses lower than a critical threshold stress. This limiting stress is composition-dependent,[74] increasing for decreasing PT content, but always of the order of 10 MPa. After the threshold stress, there is a large hysteresis which saturates at high stresses

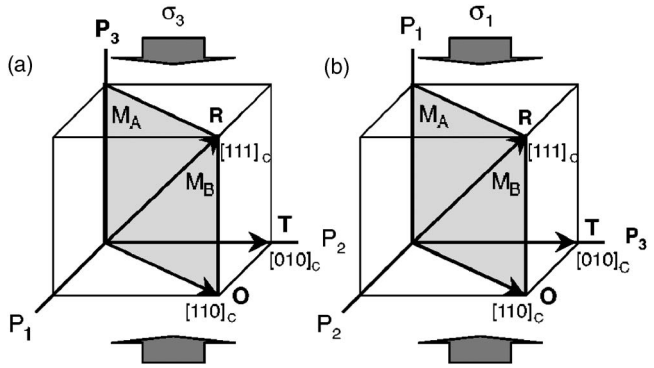

FIG. 14. Schematic illustration of a single rhombohedral domain variant with polarization **P** along $[111]_C$ under compressive stress. In our model, application of the stress will lead to a R-M_B-O rotation. In the longitudinal mode (a), the polar vector will rotate away from the P_3 poling direction. In the transverse mode (b), the rotation is toward the P_3 poling direction.

(>60 MPa).[43] The reciprocal gradient at high compressive stress tends to small values of d_{33}. Moreover, the loops are never closed. Depolarizations ΔD_3 of the order of −0.1 C/m^2 are observed for all compositions. For the response of PZN-4.5PT presented here [Fig. 13(b)], the depolarization is in fact an order of magnitude smaller suggesting that the depoling effect might be smaller at lower PT contents in PMN-xPT and PZN-xPT.

Although no explanation for the behavior was offered by Feng *et al.*, Wan *et al.* suggested an underlying stress-induced phase transition[43] (SIPT). Perhaps a more obvious explanation for the hysteresis would be global ferroelastic switching. The behavior observed is indeed qualitatively similar to the charge-stress response of soft PZT polycrystalline ceramics,[41] where ferroelastic switching can be expected. However, as discussed here and elsewhere,[11,43] the domain-engineered structure formed in $[001]_C$-poled rhombohedral PMN-xPT and PZN-xPT precludes any domain wall contribution to the direct piezoelectric response under application of a uniaxial stress σ_3. Furthermore, there are significant differences between the behavior of domain-engineered, $[001]_C$-oriented PZN-4.5PT [Fig. 13(b)], where no ferroelastic contribution is expected, and $[111]_C$-oriented PZN-4.5PT, where non-180° domain switching is expected [Fig. 12(b)]. Finally, following a single charge-stress loading (unloading) cycle in $[111]_C$-oriented PZN-4.5PT, the room temperature dielectric constant was found to increase significantly (by 40%) from 710 after poling to 1010 indicating a significant reduction in the number of c domains (depoling). In the case of $[001]_C$-poled PZN-4.5PT after repeated loading and unloading, the dielectric constant changed little (by 5%) from 4970 after poling to 4730.

In their paper, Wan *et al.* suggested a stress-induced phase transition from a rhombohedral phase to either an orthorhombic or tetragonal phase via intermediate monoclinic phases,[43] although this was not confirmed by HRD. The results presented here fit well with their hypothesis. The situation is shown schematically in Fig. 14(a) for one of the four domain variants in the domain-engineered structure. We assume in this schematic that the polar vector in each of the

four domain variants can rotate freely, independent of the other three, and we do not consider the domain structure. At zero stress, the rhombohedral polar vector is defined by $P_1 = P_2 = P_3$. Upon application of a compressive stress σ_3 along the $[001]_C$-poling direction, the polar vector $\mathbf{P}=(P_1,P_2,P_3)$ will rotate away from $[001]_C$ in the $M_B(1\bar{1}0)_C$ monoclinic plane. Due to the symmetry of the loading conditions in this simple, single-variant model, the condition $P_1=P_2$ should hold, suggesting that the simplest rotation path R-M_B-O will be followed. In this case, the reciprocal gradient measured at zero stress (1550 pC/N) will correspond to d_{33} of the pseudorhombohedral phase for polarization rotation in the M_B plane. Under high compressive stresses, the reciprocal gradient should correspond to d_{22} of the final orthorhombic phase, i.e., zero. The reciprocal gradient does indeed tend to zero at high stresses, as shown in Fig. 13(b). However, since the same would be true of an induced tetragonal phase ($d_{22}=0$), a HRD study is needed to confirm the polarization path, and the final induced phase.

Importantly, the hysteretic charge-stress response suggests that the polarization rotation involves a first-order-like jump of the polar vector within the M_B monoclinic plane, or between monoclinic planes if a tetragonal phase is induced. Such a stress-induced phase transition would indeed fit well with the results of Viehland and Powers.[44] There, strain loops measured as a function of compressive stress for $[001]_C$-oriented PMN-30PT single crystals have features very similar to those for the charge-stress loop presented here.[44] Most interestingly, the application of a bias electric field along $[001]_C$ tended to remove the hysteresis. In the stress-induced phase transition model, the bias electric field will act oppositely to the compressive stress leading to a larger threshold stress for the phase transition.

The transverse response shown in Fig. 13(a) can also be explained by a stress-induced phase transition. For the simple, single-variant model, the loading conditions are completely analogous [Fig. 14(b)] and the R-M_B-O rotation is again expected. The hysteresis and discontinuity in the charge-stress loop suggests a first-order-like phase transition. In this case, however, the reciprocal gradients are different. At zero stress, the reciprocal gradient corresponds to the d_{31} of the domain-engineered rhombohedral structure. $d_{31} = -1290$ pC/N measured here is higher than those made both by the converse piezoelectric (−850 pm/V)[35] and resonance measurements (−970 pm/V)[75] reported elsewhere for PZN-4.5PT. At high stress, the reciprocal gradient does not tend to zero, but instead tends to a finite value of −170 pC/N. This will correspond to $d_{32}(\neq d_{31})$ of the induced orthorhombic phase or $d_{31}(=d_{32})$ of the tetragonal phase. Note that the negative sign of the high field gradient is consistent with the d_{32} of other orthorhombic perovskites, which is commonly negative.[76]

The most important difference between the two loading modes is that in the transverse case, the loop is closed, with no depolarization, indicating complete reversibility of the R-M_B-O path. Similarly closed, transverse mode, charge-stress loops have been reported by McLaughlin *et al.* for compressive stresses applied perpendicular to a $[101]_C$-oriented sample[45] of PMN-32PT. In contrast, for the longitudinal measurements observed here and elsewhere,[43,74] the loops are not closed and net depolarization is observed upon unloading. The difference in behaviors agrees well with work presented previously on the dynamic, low stress (<20 MPa), direct response of $[001]_C$ PZN-4.5PT and PMN-32PT (Refs. 11 and 77). There, the transverse response was found to be anhysteretic and linear whereas the direct effect was found to be hysteretic and nonlinear. Longitudinal stresses applied along the $[001]_C$-poling direction tended to depole the samples, whereas stresses applied perpendicular to the $[001]_C$ direction tended to better pole the samples.[77] Depoling by ferroelastic switching is not expected in a rhombohedral domain-engineered structure under application of a compressive stress along $[001]_C$.[11,43]

Wan *et al.* explained the remnant strain and polarization in the longitudinal case by the presence of remnant tetragonal (though not orthorhombic) domains. For PMN-32PT (Ref. 43), the remnant polarization after loading to −60 MPa was found to be around -0.13 C/m^2 and the remnant strain was −0.07%. In our paper,[11] we postulated that the difference was related to a different direction of polarization rotation (rather than, say, a different polarization rotation path). For rotation toward the poling direction, the response is linear and anhysteretic; for rotation away from the poling direction, the response is hysteretic and nonlinear. This can be examined with further reference to the simple R-M_B-O polarization rotation model (Fig. 14). The two loading conditions are in fact analogous. In the longitudinal case [Fig. 14(a)], we apply a stress along the 3 (poling) direction, such that symmetry fixes $P_1=P_2$ and the rotation is in the dodecahedral monoclinic plane, and measure the P_3 component of polarization. In the transverse case [Fig. 14(b)], we apply stress along the 1 direction, this time fixing $P_2=P_3$, and measure the polarization P_3 along the poling direction. The difference between the two situations is that in the transverse mode, the final orthorhombic structure is domain engineered with respect to the poling direction (P_3), whereas in the resultant structure, in the longitudinal case, it is not. Any remnant orthorhombic domains in the longitudinal case after unloading will lead to a net depolarization and a net remnant compressive strain. Remnant orthorhombic (or tetragonal) domains in the transverse case will not and might even lead to a net poling effect. Likewise, if the reverse path O-M_B-R proceeds in the opposite direction upon removal of the longitudinal stress, a net depolarization will result. This cannot occur in the domain-engineered transverse case.

Moreover, this important difference between the transverse and longitudinal behaviors will have distinct consequences for the use of PMN-xPT and PZN-xPT single crystals in sensing applications. Where linear, anhysteretic behavior is required and a small sacrifice in responsiveness can be made (d_{31} is around half the magnitude of d_{33} in $[001]_C$ crystals), the transverse mode should be used. Although both modes become hysteretic after a critical stress of around 10 MPa, due to a stress-induced phase transition, this does not lead to depoling in the transverse mode.

Finally, it should be reiterated that this stress-induced phase transition remains to be verified by an *in situ* structural study, by polarized light microscopy, x-ray diffraction, or

otherwise. However, by analogy to those induced by changes in electric field, a wide range of such stress-induced phase transitions should be possible in PZN-xPT and PMN-xPT. Moreover, they should occur at relatively weak perturbing stresses, especially near the MPB where phases are nearly degenerate.

V. CONCLUSIONS

Various electric-field-induced phase transitions have been evidenced by macroscopic strain-field measurements in $[001]_C$-poled PZN-xPT and PMN-xPT with various compositions around the morphotropic phase boundary. Unipolar electric fields up to 1500 V/mm have been applied at temperatures between 25 °C and 100 °C. For lower lead titanate (PT) contents (PMN-25PT), the polarization rotation path pseudorhombohedral (R/M_A)–tetragonal (T) is followed. Here, the polar vector rotates continuously in the M_A monoclinic plane before a first-order-like, hysteretic jump within the same monoclinic plane to a tetragonal phase. At higher PT contents (PZN-5PT, PZN-6.5PT, PMN-30.5PT, PMN-31PT), the polarization rotation path is pseudorhombohedral (M_A)–pseudo-orthorhombic (M_C)–tetragonal (T). This more complicated path involves continuous rotation within the M_A plane before a first-order, hysteretic jump to the M_C monoclinic plane, continuous rotation within this second plane, and finally a second, first-order, hysteretic jump to the tetragonal phase. Both first-order phase transitions can be observed within the same electric-field cycle. At even higher PT contents (PZN-8.5PT), the zero-field phase is already pseudo-orthorhombic and only the M_C-T phase transition occurs.

Trends in phase stability have been highlighted by constructing electric-field-temperature phase diagrams for each composition. The M_C phase field is noticeably squeezed out at lower PT contents. Both M_C and tetragonal fields are favored over the M_A phase by increases in temperature and electric field along $[001]_C$. The question of whether the monoclinic phases are true ground state (zero-field) phases has been considered; it is noted that the above behavior can be explained simply in terms of first-order phase transitions between electric-field distorted rhombohedral, orthorhombic, and tetragonal phases. However, irrespective of whether it corresponds to a true monoclinic phase or simply the piezoelectric distortion of higher symmetry rhombohedral and orthorhombic parents, it is the rotation of the polar vector in the M_A and M_C monoclinic planes that is responsible for the giant piezoelectric response. Such polarization rotations are commonly large where two ferroelectric phases are nearly degenerate,[52] for example, near a morphotropic phase boundary,[33] but uncommonly large in relaxor ferroelectric PMN-xPT and PZN-xPT.

Furthermore, an analogous stress-induced phase transition has been evidenced in direct piezoelectric measurements of $[001]_C$-poled PZN-4.5PT under the application of a stress both along and perpendicular to the poling direction. The results suggest a rhombohedral-orthorhombic transition path via polarization rotation in the M_B monoclinic plane (R-M_B-O), although this remains to be confirmed by an *in situ* structural study. A first-order-like, hysteretic jump is evident within the M_B plane. Where the compressive stress is applied along the $[001]_C$-poling direction, the induced phase is not domain engineered with respect to that direction and net depolarization occurs upon unloading. In contrast, when a stress is applied perpendicular to the $[001]_C$-poling direction, the resultant orthorhombic structure is domain engineered with respect to $[001]_C$ and does not depolarize upon unloading.

Finally, such transitions between phases are a common feature of PZN-xPT and PMN-xPT around the morphotropic phase boundary, even for small changes in temperature, electric field, or stress; this follows from their near degeneracy.

ACKNOWLEDGMENTS

The authors wish to acknowledge financial support from the Swiss National Science Foundation. We are also grateful to Professor L. C. Lim at Microfine Technologies for supplying us with samples of PZN-xPT.

[1] S. E. E. Park and W. Hackenberger, Curr. Opin. Solid State Mater. Sci. **6**, 11 (2002).
[2] B. Noheda, Curr. Opin. Solid State Mater. Sci. **6**, 27 (2002).
[3] J. Kuwata, K. Uchino, and S. Nomura, Ferroelectrics **37**, 579 (1981).
[4] O. Noblanc, P. Gaucher, and G. Calvarin, J. Appl. Phys. **79**, 4291 (1996).
[5] Y. Uesu, M. Matsuda, Y. Yamada, K. Fujishiro, D. E. Cox, B. Noheda, and G. Shirane, J. Phys. Soc. Jpn. **71**, 960 (2002).
[6] A. K. Singh and D. Pandey, Phys. Rev. B **67**, 064102 (2003).
[7] V. A. Shuvaeva, A. M. Glazer, and D. Zekria, J. Phys.: Condens. Matter **17**, 5709 (2005).
[8] J. M. Kiat, Y. Uesu, B. Dkhil, M. Matsuda, C. Malibert, and G. Calvarin, Phys. Rev. B **65**, 064106 (2002).
[9] S. E. E. Park and T. R. Shrout, J. Appl. Phys. **82**, 1804 (1997).
[10] B. Jaffe, W. R. Cook, Jr., and H. Jaffe, *Piezoelectric Ceramics* (Academic, New York, 1971).
[11] M. Davis, D. Damjanovic, and N. Setter, J. Appl. Phys. **95**, 5679 (2004).
[12] Y. Lu, D. Y. Jeong, Z. Y. Cheng, Q. M. Zhang, H. S. Luo, Z. W. Yin, and D. Viehland, Appl. Phys. Lett. **78**, 3109 (2001).
[13] S. Priya, J. Ryu, L. E. Cross, K. Uchino, and D. Viehland, Ferroelectrics **274**, 121 (2002).
[14] D. Vanderbilt and M. H. Cohen, Phys. Rev. B **63**, 094108 (2001).
[15] D. H. Lee and N. K. Kim, Mater. Lett. **34**, 299 (1998).
[16] A. A. Bokov, H. Luo, and Z. G. Ye, Mater. Sci. Eng., B **120**, 206 (2005).
[17] D. La-Orauttapong, J. Toulouse, Z. G. Ye, W. Chen, R. Erwin, and J. L. Robertson, Phys. Rev. B **67**, 134110 (2003).
[18] Z. G. Ye, Y. Bing, J. Gao, A. A. Bokov, P. Stephens, B. Noheda, and G. Shirane, Phys. Rev. B **67**, 104104 (2003).
[19] Z. G. Ye and M. Dong, J. Appl. Phys. **87**, 2312 (2000).

[20] K. Fujishiro, R. Vlokh, Y. Uesu, Y. Yamada, J. M. Kiat, B. Dkhil, and Y. Yamashita, Jpn. J. Appl. Phys., Part 1 **37**, 5246 (1998).
[21] M. Matsushita, Y. Tachi, and K. Echizenya, J. Cryst. Growth **237**, 853 (2002).
[22] H. Luo, G. Xu, H. Xu, P. Wang, and Z. Yin, Jpn. J. Appl. Phys., Part 1 **39**, 5581 (2000).
[23] F. Bai, N. Wang, J. Li, D. Viehland, P. M. Gehring, G. Xu, and G. Shirane, J. Appl. Phys. **96**, 1620 (2004).
[24] K. Ohwada, K. Hirota, P. W. Rehrig, Y. Fujii, and G. Shirane, Phys. Rev. B **67**, 094111 (2003).
[25] H. Cao, F. Bai, N. Wang, J. Li, D. Viehland, G. Xu, and G. Shirane, Phys. Rev. B **72**, 064104 (2005).
[26] A. J. Bell, J. Appl. Phys. **89**, 3907 (2001).
[27] M. Davis, D. Damjanovic, and N. Setter, J. Appl. Phys. **96**, 2811 (2004).
[28] M. Davis, D. Damjanovic, and N. Setter, J. Appl. Phys. **97**, 064101 (2005).
[29] B. Noheda, Z. Zhong, D. E. Cox, G. Shirane, S. E. Park, and P. Rehrig, Phys. Rev. B **65**, 224101 (2002).
[30] B. Noheda, D. E. Cox, G. Shirane, S. E. Park, L. E. Cross, and Z. Zhong, Phys. Rev. Lett. **86**, 3891 (2001).
[31] E. H. Kisi, R. O. Piltz, J. S. Forrester, and C. J. Howard, J. Phys.: Condens. Matter **15**, 3631 (2003).
[32] A. Amin, M. J. Haun, B. Badger, H. McKinstry, and L. E. Cross, Ferroelectrics **65**, 107 (1985).
[33] M. J. Haun, E. Furman, S. J. Jang, and L. E. Cross, Ferroelectrics **99**, 13 (1989).
[34] H. Fu and R. E. Cohen, Nature (London) **403**, 281 (2000).
[35] S. F. Liu, S. E. Park, T. R. Shrout, and L. E. Cross, J. Appl. Phys. **85**, 2810 (1999).
[36] W. Ren, S. F. Liu, and B. K. Mukherjee, Appl. Phys. Lett. **80**, 3174 (2002).
[37] R. Chien, V. H. Schmidt, C. S. Tu, L. W. Hung, and H. Luo, Phys. Rev. B **69**, 172101 (2004).
[38] M. K. Durbin, E. W. Jacobs, and J. C. Hicks, Appl. Phys. Lett. **74**, 2848 (1999).
[39] D. Viehland and J. F. Li, J. Appl. Phys. **92**, 7690 (2002).
[40] S. Wada, S. Suzuki, T. Noma, T. Suzuki, M. Osada, M. Kakihana, S. E. Park, L. E. Cross, and T. R. Shrout, Jpn. J. Appl. Phys., Part 1 **38**, 5505 (1999).
[41] C. S. Lynch, Acta Mater. **44**, 4137 (1996).
[42] M. N. Shetty, V. C. S. Prasad, and E. C. Subbarao, Phys. Rev. B **10**, 4801 (1974).
[43] Q. Wan, C. Chen, and Y. P. Shen, J. Appl. Phys. **98**, 024103 (2005).
[44] D. Viehland and J. Powers, J. Appl. Phys. **89**, 1820 (2001).
[45] E. A. McLaughlin, T. Liu, and C. S. Lynch, Acta Mater. **52**, 3849 (2004).
[46] D. Zekria, V. A. Shuvaeva, and A. M. Glazer, J. Phys.: Condens. Matter **17**, 1593 (2005).
[47] S. W. Choi, T. R. Shrout, S. J. Jang, and A. S. Bhalla, Ferroelectrics **100**, 29 (1989).
[48] D. Damjanovic, J. Appl. Phys. **82**, 1788 (1997).
[49] A. Barzegar, D. Damjanovic, and N. Setter, IEEE Trans. Ultrason. Ferroelectr. Freq. Control **51**, 262 (2003).
[50] S. Wada, K. Yako, H. Kakemoto, T. Tsurumi, and T. Kiguchi, J. Appl. Phys. **98**, 014109 (2005).
[51] M. Davis, D. Damjanovic, and N. Setter, Appl. Phys. Lett. **87**, 102904 (2005).
[52] M. Budimir, D. Damjanovic, and N. Setter, J. Appl. Phys. **94**, 6753 (2003).
[53] R. Zhang, B. Jiang, and W. Cao, Appl. Phys. Lett. **82**, 787 (2003).
[54] M. Shen, D. Yao, and W. Cao, Mater. Lett. **59**, 3276 (2005).
[55] M. Davis, D. Damjanovic, D. Hayem, and N. Setter, J. Appl. Phys. **98**, 014102 (2005).
[56] J. S. Forrester, R. O. Piltz, E. H. Kisi, and G. J. McIntyre, J. Phys.: Condens. Matter **13**, L825 (2001).
[57] I. A. Sergienko, Y. M. Gufan, and S. Urazhdin, Phys. Rev. B **65**, 144104 (2002).
[58] L. D. Landau and E. M. Lifshitz, *Statistical Physics Part 1*, 3rd ed. (Butterworth-Heinemann, Oxford, 1980).
[59] L. Bellaiche, A. Garcia, and D. Vanderbilt, Phys. Rev. B **64**, 060103(R) (2001).
[60] G. Xu, H. Luo, H. Xu, and Y. Yin, Phys. Rev. B **64**, 020102(R) (2001).
[61] A. A. Bokov and Z. G. Ye, J. Appl. Phys. **95**, 6347 (2004).
[62] M. K. Durbin, J. C. Hicks, S. E. Park, and T. R. Shrout, J. Appl. Phys. **87**, 8159 (2000).
[63] K. K. Rajan and L. C. Lim, Appl. Phys. Lett. **83**, 5277 (2003).
[64] V. Y. Topolov, Phys. Rev. B **65**, 094207 (2002).
[65] M. Shen and W. Cao, Appl. Phys. Lett. **86**, 192909 (2005).
[66] J. Han and W. Cao, Appl. Phys. Lett. **83**, 2040 (2003).
[67] Y. M. Jin, Y. U. Wang, and A. G. Khachaturyan, J. Appl. Phys. **94**, 3629 (2003).
[68] L. Bellaiche, A. Garcia, and D. Vanderbilt, Phys. Rev. Lett. **84**, 5427 (2000).
[69] J. Frantti, S. Eriksson, S. Hull, V. Lantto, H. Rundlöf, and M. Kakihana, J. Phys.: Condens. Matter **15**, 6031 (2003).
[70] R. Haumont, A. Al-Barakaty, B. Dkhil, J. M. Kiat, and L. Bellaiche, Phys. Rev. B **71**, 104106 (2005).
[71] B. Noheda, D. E. Cox, G. Shirane, J. A. Gonzalo, L. E. Cross, and S. E. Park, Appl. Phys. Lett. **74**, 2059 (1999).
[72] Y. Ishibashi and M. Iwata, Jpn. J. Appl. Phys., Part 1 **38**, 800 (1999).
[73] J. Yin and W. Cao, Appl. Phys. Lett. **80**, 1043 (2002).
[74] Z. Feng, D. Lin, H. Luo, S. Li, and D. Fang, J. Appl. Phys. **97**, 024103 (2005).
[75] J. Yin, B. Jiang, and W. Cao, IEEE Trans. Ultrason. Ferroelectr. Freq. Control **47**, 285 (2000).
[76] M. Zgonik, R. Schlesser, I. Biaggio, E. Voit, J. Tscherry, and P. Gunter, J. Appl. Phys. **74**, 1287 (1993).
[77] M. Davis, D. Damjanovic, and N. Setter, *Proceedings of the 14th IEEE International Symposium on Applications of Ferroelectrics* (IEEE, New York, 2004), pp. 102–105.